Product Datasheet

LC3B Antibody - BSA Free
NB600-1384

Unit Size: 0.1 ml

Aliquot and store at -20C or -80C. Avoid freeze-thaw cycles.

www.novusbio.com technical@novusbio.com

Reviews: 19 Publications: 397

Protocols, Publications, Related Products, Reviews, Research Tools and Images at:
www.novusbio.com/NB600-1384

Updated 12/20/2023 v.20.1

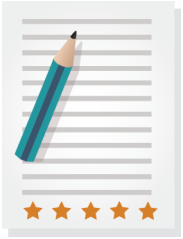

NB600-1384

LC3B Antibody - BSA Free

Product Information	
Unit Size	0.1 ml
Concentration	1.0 mg/ml
Storage	Aliquot and store at -20C or -80C. Avoid freeze-thaw cycles.
Clonality	Polyclonal
Preservative	0.02% Sodium Azide
Isotype	IgG
Purity	Immunogen affinity purified
Buffer	PBS
Target Molecular Weight	14.688 kDa

Product Description	
Host	Rabbit
Gene ID	81631
Gene Symbol	MAP1LC3B
Species	Human, Mouse, Rat, Porcine, Bacteria, Bovine, Canine, Primate, Yeast, Zebrafish
Reactivity Notes	Use in Yeast reported in scientific literature (PMID:35247568).Use in Rat reported in scientific literature (PMID:34499623). Mouse reactivity reported in scientific literature (PMID:32802192). Zebrafish reactivity reported in scientific literature (PMID: 23724125). . Canine and primate reactivity reported in scientific literature (PMID: 24027311). Porcine reactivity reported in scientific literature (PMID: 25378587). . Rat reactivity reported in scientific literature (30067379). . Bacteria reactivity reported in scientific literature (31110360). . Bovine reactivity reported in scientific literature (21868124). . Other species have not been tested.
Marker	Autophagosome Marker
Immunogen	Polyclonal LC3B Antibody was made to a synthetic peptide made to the N-terminal region of the human LC3B protein. [Uniprot: Q9GZQ8]

Product Application Details	
Applications	Western Blot, Simple Western, Electron Microscopy, Flow Cytometry, Immunoblotting, Immunocytochemistry/ Immunofluorescence, Immunohistochemistry, Immunohistochemistry-Frozen, Immunohistochemistry-Paraffin, Immunoprecipitation, Immunohistochemistry Free-Floating, Knockdown Validated, Knockout Validated
Recommended Dilutions	Western Blot 1:1000, Simple Western 1:100, Flow Cytometry 1:200, Immunohistochemistry, Immunocytochemistry/ Immunofluorescence, Immunoprecipitation, Immunohistochemistry-Paraffin 1:200-1:400, Immunohistochemistry-Frozen 1:400, Immunoblotting, Electron Microscopy, Immunohistochemistry Free-Floating, Knockout Validated, Knockdown Validated

Application Notes	In Western Blot, bands are seen at ~17 and 19 kDa corresponding to LC3-II and LC3-I. The observed molecular weight of the protein may vary from the listed predicted molecular weight due to post translational modifications, post translation cleavages, relative charges, and other experimental factors. Electron Microscopy was reported in scientific literature (PMID: 21885071). Use in Immunohistochemistry-free floating reported in scientific literature (PMID: 24928515). Use in Immunohistochemistry on both paraffin-embedded and frozen sections reported in scientific literature (PMID: 18259115). Use in immunoprecipitation reported in scientific literature (PMID: 26098573). Use in immunoblotting reported in scientific literature (PMID: 25383539). Use in flow reported in scientific literature (PMID: 27622036). In Simple Western only 10 - 15 uL of the recommended dilution is used per data point. Separated by Size-Wes, Sally Sue/Peggy Sue.

Images

FTC-133/TPC-1 cells were transfected with HMGB1 shRNA and control shRNA and then pre-treated for 1 h with pepstatin A (PA, 10 uM) and E64D (10 uM) as indicated. Cells were subsequently treated for 3 h with HBSS in continuous presence or absence PA/E64D inhibitors. LC3-I/II levels were assayed by Western blot. Image collected and cropped by CiteAb from the following publication (https://jeccr.biomedcentral.com/articles/10.1186/s13046-019-1328-3) licensed under a CC-BY license.	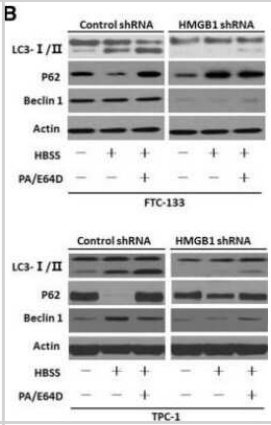
Analysis of LC3B in HeLa cells using anti-LC3B antibody (red) [Catalog # NB600-1384]. Nuclei were counterstained with DAPI (blue).	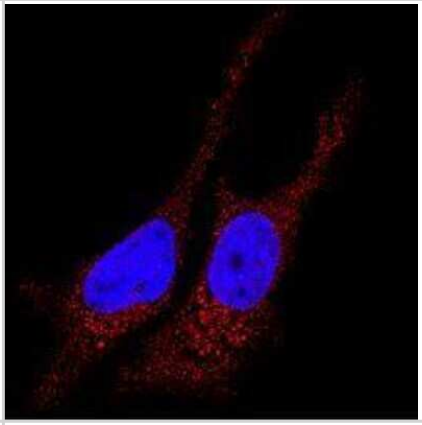
LC3B immunohistochemical staining in CC tissue(A) CC with low LC3B dot like staining. (B) CC with high LC3B dot like staining. (magnification 20X). Image collected and cropped by CiteAb from the following publication (https://www.oncotarget.com/lookup/doi/10.18632/oncotarget.17554) licensed under a CC-BY license.	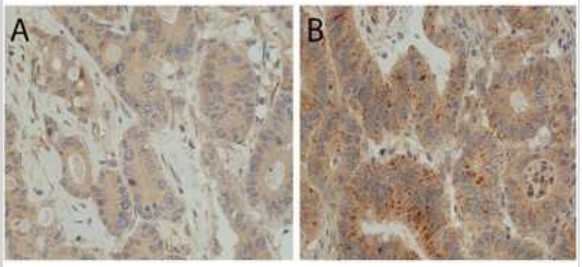

Analysis of LC3B in treated U87-MG (human glioblastoma astrocytoma) lysates using anti- [Catalog # NB600-1384].	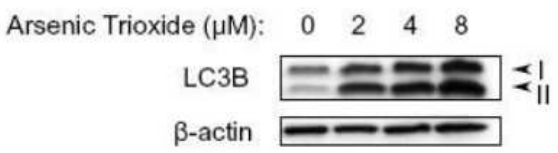
Depletion of RARalpha prevents ATRA-induced autophagic flux in SKBR3 cells. LC3B western blotting and quantification of the autophagic activity in control and RARalpha-knockdown SKBR3 cells upon treatment with 1 uM ATRA for 2 days in the presence or absence of BafA for 2 h at 200 nM. LC3B-II expression was normalized to GAPDH and to vehicle-treated control cells. Standard deviations from at least five independent experiments are shown. Image collected and cropped by CiteAb from the following publication (https://www.nature.com/articles/cddis2015236), licensed under a CC-BY license.	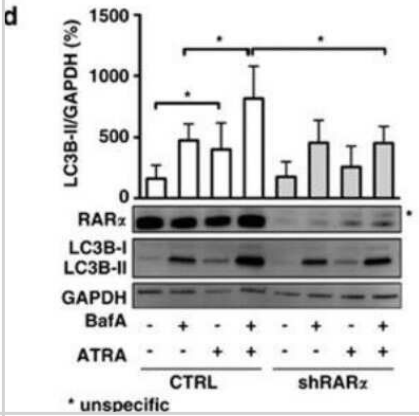
Human cervical carcinoma (HeLa) and Mouse Neuroblast cells (Neuro2a) were treated with (+) and without (-) 50 uM Chloroquine overnight. Whole cell protein lysates were prepared in 1x Laemmli sample buffer and approximately 10 ug of each lysate (NBP2-49689 and NBP2-49688) was separated on a 4- 20% gel by SDS-PAGE, transferred to 0.2 um PVDF membrane and blocked in 5% nonfat milk in TBST. The membrane was probed with 2 ug/mL anti-LC3 (NB600-1384) and 1 ug/mL anti-alpha tubulin (NB100-690) as a loading control, and detected with the appropriate secondary antibodies using NovaLume Pico Chemiluminescence Substrate (NBP2-61915).	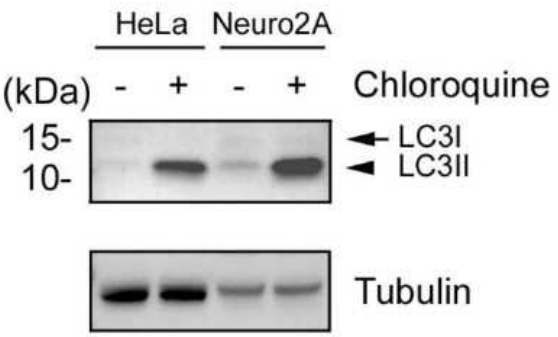
Fibroblasts were exposed to 1 mM LLOMe and when indicated pretreated with the autophagy inhibitors 3-methyladenine (5 mM, 1 h) or bafilomycin A1 (25 nM, 30 min). Immunostaining with corresponding colocalization analysis of a) LC3 (green) and galectin-3 (red) and b) LC3 (green) and LAMP2 (red). Merged images show colocalization in yellow, nuclei are stained with DAPI (blue). LLOME = l-leucyl-l-leucine methyl ester, a lysosomal membrane damage compound. Image collected and cropped by CiteAb from the following publication (//pubmed.ncbi.nlm.nih.gov/32409651/) licensed under a CC-BY license.	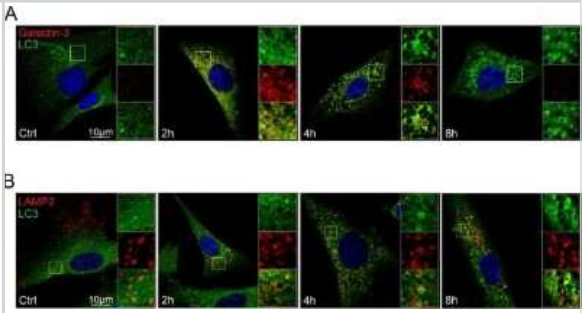

Confocal analysis of HeLa cells using Rabbit anti-LC3B antibody (Catalog # NB600-1384, 1:5). An Alexa Fluor 488-conjugated Goat to rabbit IgG was used as secondary antibody (green). Actin filaments were labeled with Alexa Fluor 568 phalloidin (red). DAPI was used to stain the cell nuclei (blue).	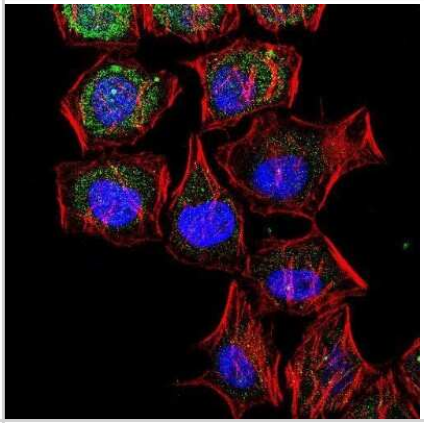
Immunocytochemical/Immunofluorescent staining of treated U373-MG cells using the HRP conjugate of anti- (Catalog # NB600-1384). The nuclei were stained with DAPI.	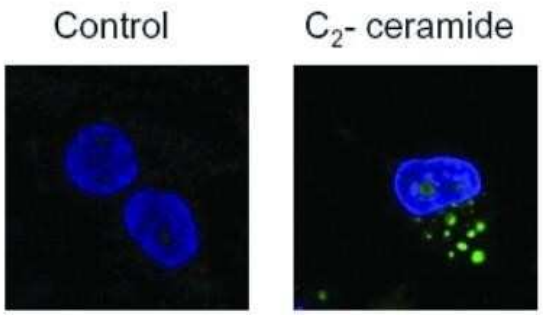
Staining of treated U373-MG (human glioblastoma) cells using anti- [Catalog # NB600-1384].	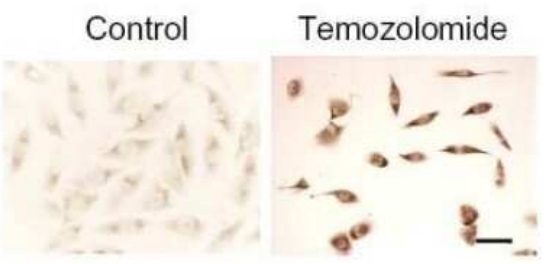
Analysis of U87MG glioma xenografts using anti- [Catalog # NB600-1384]. Image from verified customer review.	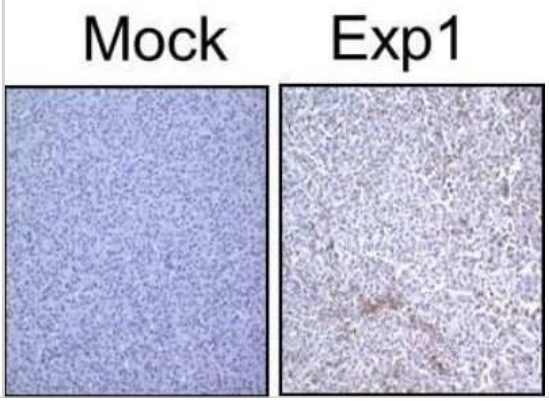

LC3B staining in treated U87-MG cultured & subcutaneous tumors.	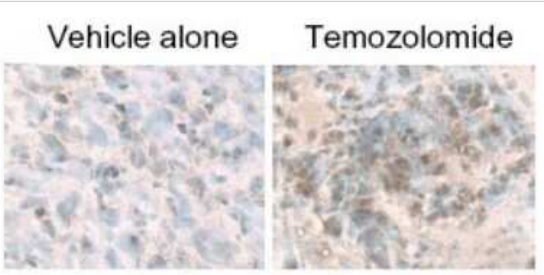
LC3B staining in glioblastoma multiform tissue.	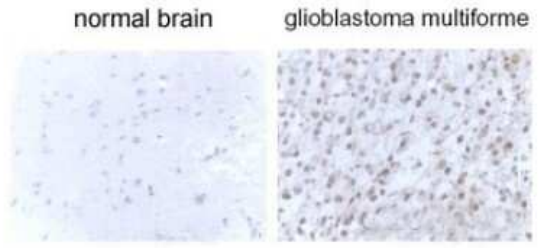
Lane view shows a specific band for LC3B in 0.5 mg/ml of Neuro2A lysate at a molecular weight of approximately 15 kDa. This experiment was performed under reducing conditions using the 12-230 kDa separation system.	
LC3A and LC3B siRNAs specifically block the expression of the LC3A and LC3B proteins, respectively, in A549 cell line (E1,2,3). In E4 the reactivity of and of the LC3B (5F10 antibody) is shown, following silencing of the LC3A or of the LC3B genes, in the A549 cell line. Image collected and cropped by CiteAb from the following publication (https://dx.plos.org/10.1371/journal.pone.0137675), licensed under a CC-BY license.	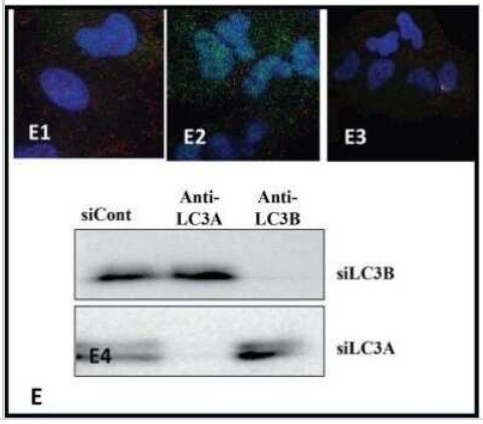

NOD1-dependent induction of autophagy contributes to IRGM and LC3 recruitment to Mtb-containing vesicles. The subcellular localization of autophagy proteins was observed in untreated (A, C) and Tri-DAP treated cells (B, D) using anti-IRGM and anti-LC3 antibodies, which were detected using a secondary antibody coupled to 5 nm gold particles (indicated with arrowheads; TEM X 62,000). Gold particles colocalizing with bacteria were manually counted in 10 macrophages of each condition (E, F) and the differences between the treatments are indicated: ***p < 0.01 and *p < 0.05 vs. Mtb, ++p < 0.01 vs. Tri-DAP, Wilcoxon Rank test. Box plots indicate median and quartiles. Image collected and cropped by CiteAb from the following publication (https://bmcpulmmed.biomedcentral.com/articles/10.1186/1471-2466-14-152), licensed under a CC-BY license.

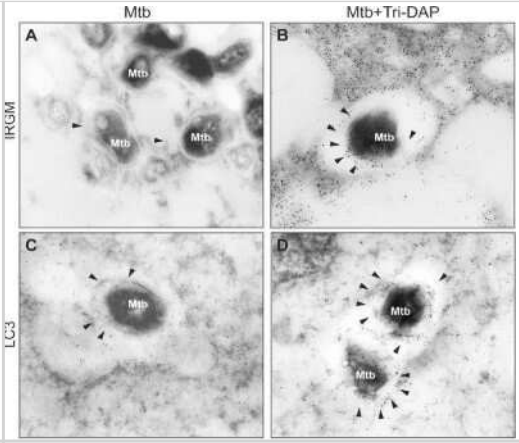

Examples of immunohistochemical stainings; (A) LC3B low, (B) LC3B high, (C) p62 low (any cellular compartment), (D) p62 cytoplasmic low, (E) p62 cytoplasmic/dot like high, nuclear low, (F) p62 cytoplasmic/dot like low, nuclear high, (G) HMGB1 low, (H) HMGB1 high. Objective magnification, 40×.

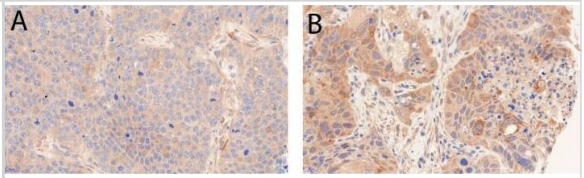

Validation of modulations in autophagy-related markers after SIRT6 knockdown in melanoma cells. (B) Western blot analyses of various autophagy markers including LC3 I and II, BECN1, SQSTM1, ATG3, ATG7, ATG10 and GAA using cell lysates of shNS and shSIRT6 in A375 melanoma cells. beta-actin was used as loading control. The figure shows representative western blot images from 2-3 experiments. Image collected and cropped by CiteAb from the following publication (https://www.genesandcancer.com/lookup/doi/10.18632/genesandcancer.153), licensed under a CC-BY licence.

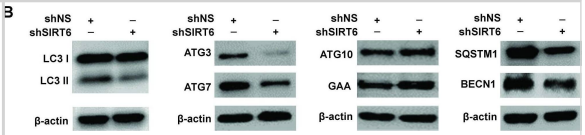

Induction of autophagic flux in OE19 upon Lapatinib treatment. (a) LC3B flux was assessed comparing control and BafilomycinA (BafA)-treated (200 nM, 2 h) OE19 upon Lapatinib treatment (120 nM, 24 h). LC3 band intensities were quantified using ImageJ software. Total protein was used as a loading control, and Phospho-Her2 for Lapatinib treatment (n = 3). Image collected and cropped by CiteAb from the following publication (https://pubmed.ncbi.nlm.nih.gov/30297650), licensed under a CC-BY licence.

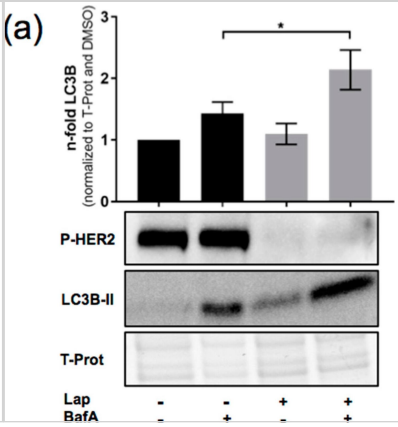

In vitro alphaS seeds induce endo-lysosome-free and endo-lysosome-associated alphaS inclusions in H4/V1S-SV2 cells. (d) The treated cells were further subjected to immunocytochemical staining of LAMP1 (Alexa fluor 405) and LC3 (Alexa fluor 568) to demonstrate the association between autophagosomes, endo-lysosomes, and seeded alphaS inclusions. Scale bar: 5 um (top row) and 2 um (bottom row). Image collected and cropped by CiteAb from the following publication (https://www.nature.com/articles/s41598-017-08149-w), licensed under a CC-BY licence.

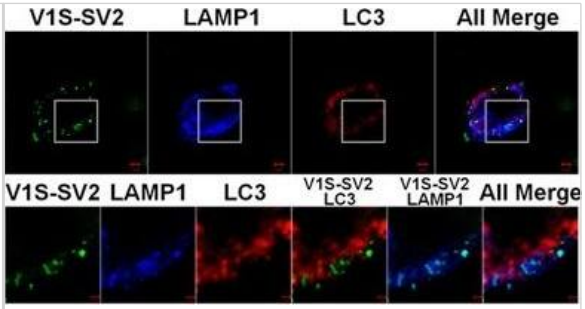

(E) LC3A and LC3B siRNAs specifically block the expression of the LC3A and LC3B proteins, respectively, in A549 cell line (E1,2,3). In E4 the reactivity of LC3A (ab62720 Ab) and of the LC3B (5F10 antibody) is shown, following silencing of the LC3A or of the LC3B genes, in the A549 cell line. Image collected and cropped by CiteAb from the following publication (https://pubmed.ncbi.nlm.nih.gov/26378792), licensed under a CC-BY licence.

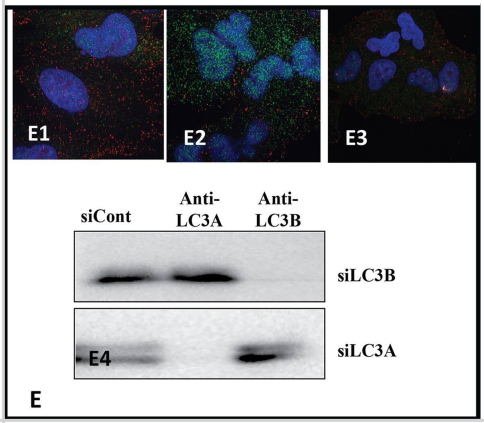

Combination treatment of valproic acid (VPA) and doxorubicin (DOX) synergistically augmented the autophagy of HepG2 cells. (D) LC3 I and II protein levels were analyzed using Western blotting. Actin was used as the loading control. The intensity of LC3B-II bands was quantified by scanning densitometry program ImageJ and normalized to that of actin (right panel). Three independent experiments were performed and results reported as the mean +/- standard deviation (SD). ** $p < 0.01$, *** $p < 0.001$ compared with the control group. Image collected and cropped by CiteAb from the following publication (https://www.mdpi.com/1422-0067/18/5/1048), licensed under a CC-BY licence.

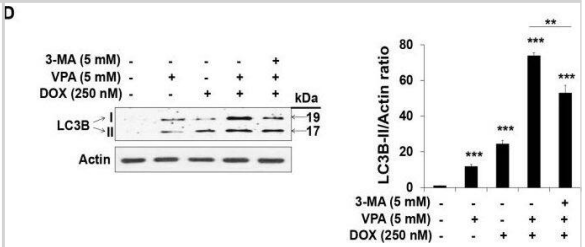

Autophagy and the proteasome regulate CagA stability. (A) Wild-type (WT) and autophagy-deficient (Atg5-/-) MEFs were infected with a CagA + vacA- isogenic mutant strain (MOI 100) for 8 hours using a gentamycin protection assay. The autophagy marker LC3-II was used to confirm that Atg5-/- MEFs are autophagy-deficient. CagA protein levels were measured by Western blotting using beta-actin as loading control. Graph shows fold change of CagA normalized to beta-actin relative to WT MEFs (mean + SEM; n = 4). Image collected and cropped by CiteAb from the following publication (https://pubmed.ncbi.nlm.nih.gov/30631092), licensed under a CC-BY licence.

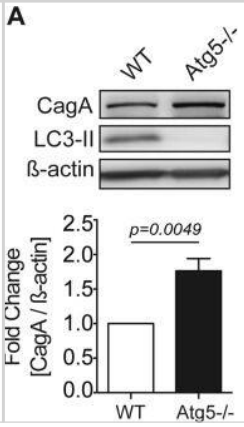

PB induces autophagy but blocks autophagosome trafficking and autophagosome-lysosome fusion in Hep3B cells. (B) Hep3B cells were treated for 6, 24 and 48 h with the indicated concentrations of PB. Levels of protein expression were analysed by Western blot using antibodies against LC3B, p62/SQSTM1, ATG12, BECN1 and Actin. Images were cropped from different blots run under the same experimental conditions. The original blots were attached as Supplementary Figure 3A. Image collected and cropped by CiteAb from the following publication (https://www.nature.com/articles/srep41437), licensed under a CC-BY licence.

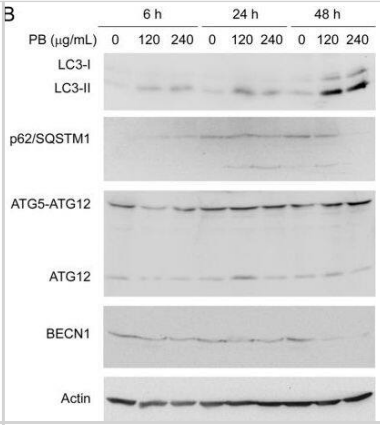

Effects of exogenous HMGB1 on ATRA-induced differentiation. E). Expression of PML-RARalpha, P62 and LC3-I/II in NB4 cells treated with ATRA (1 uM) or HMGB1 (10 ug/ml) for 48 h was assayed by western blotting and co-immunoprecipitation in comparison to control (DMSO). Image collected and cropped by CiteAb from the following publication (https://www.oncotarget.com/lookup/doi/10.18632/oncotarget.15432), licensed under a CC-BY licence.

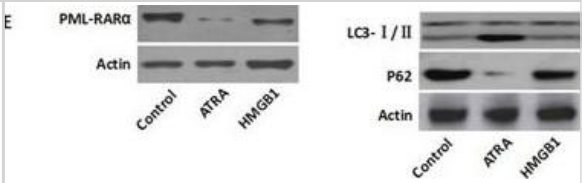

Activation of autophagy by MG132 is associated with AGR2 decline. d) The levels of AGR2 and LC3B were measured by western blotting with MG132 treatment at indicated time. e Analysis of LC3B and AGR2 accumulation in A549 cells by fluorescent staining. Scale bar = 10 um Image collected and cropped by CiteAb from the following publication (https://pubmed.ncbi.nlm.nih.gov/30647455), licensed under a CC-BY licence.

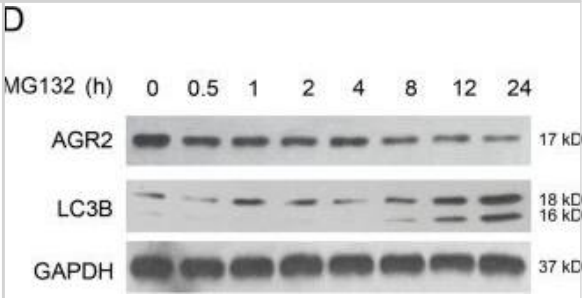

Autophagy was induced under conditions of LH and inhibited by CQ and 3-MA in HCC cells.(A-C). SMMC-7721 and HepG2 cells were directly incubated under normal or LH conditions for 8 h or incubated under LH conditions in the presence or absence of CQ or 3-MA for 8 h. (C). The whole-cell lysates were subjected to western blot analysis as described in the 'Materials and methods'section. The experiments were repeated at least three times. Image collected and cropped by CiteAb from the following publication (https://www.nature.com/articles/srep05382), licensed under a CC-BY licence.

The effect of H19 siRNA on autophagy in OGD/R model. A) Immunofluorescence of LC3II in different conditions. Image collected and cropped by CiteAb from the following publication (https://www.aginganddisease.org/EN/10.14336/AD.2016.0530), licensed under a CC-BY licence.	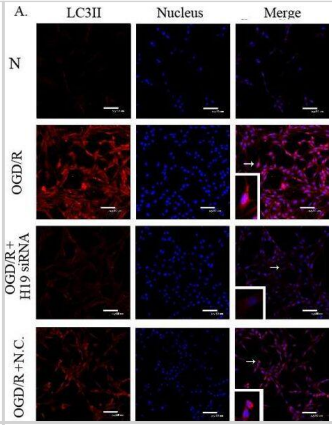
Validation of selected differentially expressed genes. A. RT-PCR analysis of genes elevated in drug resistant cells. The y-axis represents fold up-regulation in the different drug resistant cell lines over the parental OV90 cell line. B. RT-PCR analysis of genes decreased in drug resistant cells. The y-axis represents the fold down-regulation of the different resistant cell lines compared to the parental OV90 cell line. C. Immunoblot analysis of selected gene products identified by microarray and RT-PCR as altered in drug resistant cells. Image collected and cropped by CiteAb from the following open publication (https://ovarianresearch.biomedcentral.com/articles/10.1186/1757-2215-4-21), licensed under a CC-BY license. Not internally tested by Novus Biologicals.	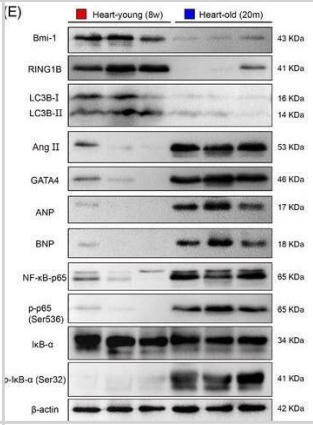
Osteogenic differentiation in 3D. (A) Histochemical staining of 12-µm-thick gel sections from one representative donor after 5 weeks of culture in undifferentiated or osteogenic conditions. Osteoimage® (HA-specific staining), von Kossa (stains anionic portion of phosphates, carbonates, and other salts) and Alizarin Red (stains Ca2+ deposits) shows differentiation in the Col I—BMSC cultures. Scale bar = 100 µm. (B) Immunostaining for osteocalcin (OCN) and nuclear 4′,6-diamidino-2-phenylindole (DAPI) in 3D cultures after 5 weeks. (C) Immunostaining for osteopontin (OPN) and nuclear DAPI in 3D cultures after 5 weeks. Scale bar = 50 µm. Image collected and cropped by CiteAb from the following open publication (https://pubmed.ncbi.nlm.nih.gov/34948393), licensed under a CC-BY license. Not internally tested by Novus Biologicals.	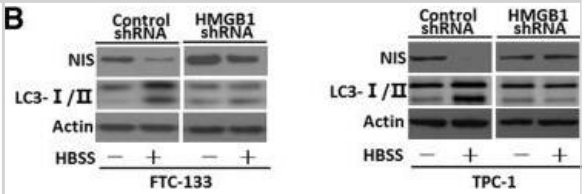

G-TPP induces PINK1 stabilization and kinase activity in HeLa cells(A) G-TPP treatment leads to PINK1 stabilization and pS65-Ub induction in HeLa cells. HeLa cells stably expressing untagged Parkin were treated with 10 μM G-TPP for the indicated times. Western blots were prepared with cell lysates and probed with antibodies against PINK1 and pS65-Ub. GAPDH served as a loading control. (B) pS65-Ub is induced in G-TPP treated cells and co-localizes with EGFP-Parkin and mitochondria. HeLa cells stably expressing EGFP-Parkin (green) were treated with 10 μM G-TPP for the indicated times and fixed. Cells were stained with antibodies against pS65-Ub (red) and the mitochondrial marker TOM20 (cyan). Scale bars correspond to 10 μM. (C) Quantification of Parkin translocation using High Content Imaging. HeLa EGFP-Parkin cells were treated for 4 or 8 h with or without 10 μM G-TPP. CCCP treatment (10 μM for 2 h) was used as a positive control. Cells were fixed, counterstained with Hoechst dye to visualize nuclei, imaged and analyzed using the ratio of cytoplasmic to nuclear EGFP signal [21]. Data was normalized to positive (2 h 10 μM CCCP treatment) and negative (2 h DMSO) controls. G-TPP significantly induced Parkin re-localization to levels similar to or beyond 2 h CCCP treatment. Shown are the mean values of three independent experiments with triplicate wells each ± SEM (one-way ANOVA with Tukey's posthoc, ***p < 0.0005). Image collected and cropped by CiteAb from the following open publication (https://www.oncotarget.com/lookup/doi/10.18632/oncotarget.22287), licensed under a CC-BY license. Not internally tested by Novus Biologicals.

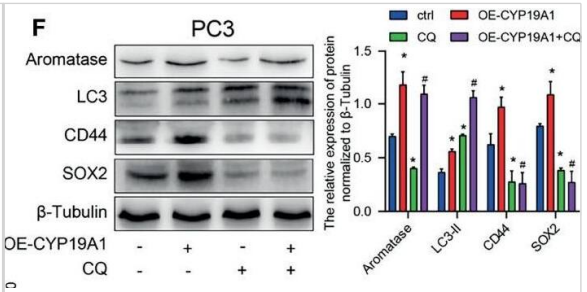

Association of p53 and APE1 on p53-binding sites in p21 promoter.(A) p21 promoter structure showing p53 and AP4 binding sites. (B) ChIP Real Time PCR analysis showing relative enrichment (2−ΔCT) of APE1-immunoprecipitated DNA over that from control IgG in p21 promoter regions containing p53 binding sites 1 & 2 in HCT116WT cells. (C) Re-ChIP analysis (first IP with α-APE1 and the second IP with α-p53 antibody) showing simultaneous recruitment of APE1 and p53 in control vs. etoposide treated cells; *: p value <0.05 (n=2) calculated based on APE1/p53 enriched DNA from control vs. etoposide treated cells. (D) Western analysis of FLAG immunoprecipitate (IP) to detect APE1-associated p53 and FLAG (APE1) from empty vector vs. FLAG-tagged WT APE1 or FLAG-tagged NΔ33 APE1 transfected HCT116WT cells (left panel) and from control vs. etoposide-treated WT APE1-FLAG transfected cells (right panel). Image collected and cropped by CiteAb from the following open publication (https://pubmed.ncbi.nlm.nih.gov/23874636), licensed under a CC-BY license. Not internally tested by Novus Biologicals.

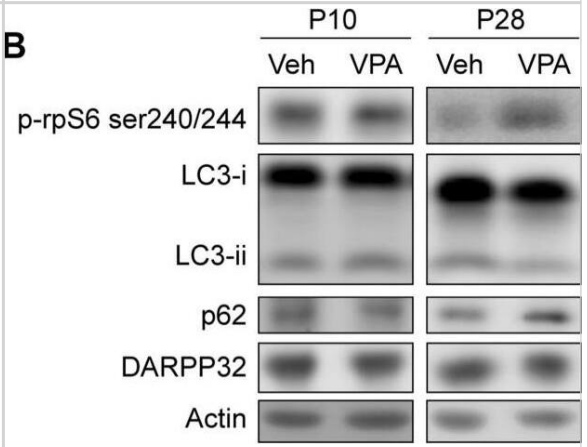

Loss of functional PRPF31 induce RNA:DNA hybrid dependent genomic instability but not in mice retinal neurons.(a andb) γH2AX and 53BP1 foci analysis in PRPF31 siRNA-transfected RPE-1 cells. (c and d) γH2AX and 53BP1 foci analysis in vasculo-stromal fraction derived primary cells fromPrpf31+/A216P mice (Prpf31-ki). (e) γH2AX and 53BP1 foci analysis in retina fromPrpf31+/A216P mice on postnatal day 20. All column bars represent the mean. For (a-d) "n", mentioned on respective column, signify number of cells analyzed from two independent experiments. For (e) n=16 for each column and signify number of retinal sections analyzed; acquired from n=4 eyes. Error bars represent Standard error of Mean (SEM). *P≤0.05; **P<0.01, ***P<0.001 using Mann-Whitney test (a,b), Kruskal-Wallis test followed by Dunn's post hoc test (c,d); and two tailed unpaired Student's t-test (e). Image collected and cropped by CiteAb from the following open publication (https://pubmed.ncbi.nlm.nih.gov/30345028), licensed under a CC-BY license. Not internally tested by Novus Biologicals.

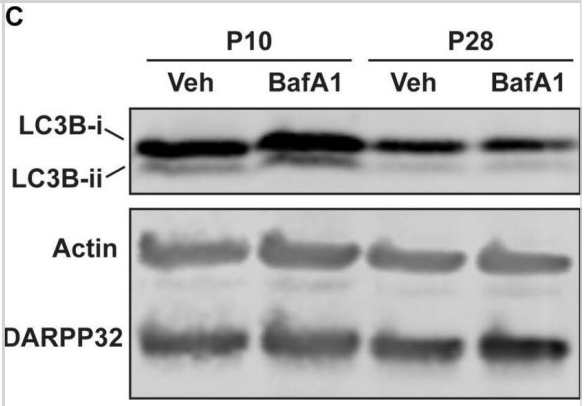

Subarachnoid hemorrhage (SAH) grades and temporal expression of endogenous osteopontin (OPN) and autophagy□related proteins in rat brain after SAH. A, Representative brain images of Sham and SAH rats. B, Summary of SAH grading scores of all groups. Sample size is 27, n = 9 per group. Data were analyzed using Kruskal□Wallis test, χ2 = 18.183. C, Representative Western blot images and quantitative analyses of OPN, Beclin 1, LC3, and ATG 5 from the left hemisphere of rat brains at different time points after SAH. Sample size is 36, n = 6 per group. Data were presented as mean ± SD. F = 28.45 for OPN, F = 12.37 for Beclin 1, F = 18.88 for LC3, F = 22.14 for ATG5. *P < .05, ** P < .01, ***P < .001 vs Sham group. SAH, subarachnoid hemorrhage; Vehicle, phosphate□buffered saline; rOPN, recombinant OPN. NS, not significant Image collected and cropped by CiteAb from the following open publication (https://pubmed.ncbi.nlm.nih.gov/31436915), licensed under a CC-BY license. Not internally tested by Novus Biologicals.

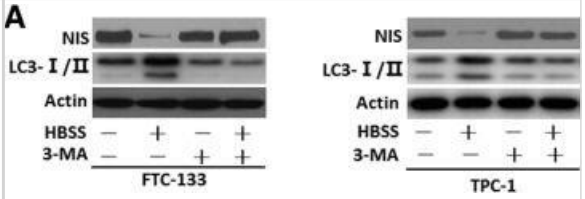

Staufen1 co-fractionates with Gag and vRNA in gradient density fractionation analyses. (A) HeLa cells were either mock transfected with empty vector, pcDNA3, or with a plasmid that expresses Staufen1-HA. The transfected cells were collected 24 h later, lysed and were either mock-treated or treated with RNAse A. The lysates were then fractionated on 5–50% sucrose gradients and 20 fractions were collected for further analysis by western blotting for viral and host proteins, as indicated. HIV-1 viral genomic RNA (vRNA, 9 kb) was assessed in each fraction by slot blot analysis. TL represents the total lysates. (B) HeLa cells were co-transfected with pNL 4–3 and Staufen1-HA. The presence of Staufen1-HA, precursor Gag and p24 were assessed in each fraction by western blotting analysis. HIV-1 viral genomic RNA (9 kb, vRNA) was assessed in each fraction by slot blot analysis. Staufen1, Gag and vRNA were quantitated in each fraction by densitometry and relative levels are depicted for each fraction (Blue: Staufen1-HA, Red: Gag, Green-vRNA). Image collected and cropped by CiteAb from the following open publication (https://journal.frontiersin.org/article/10.3389/fmicb.2012.00367/abstract), licensed under a CC-BY license. Not internally tested by Novus Biologicals.

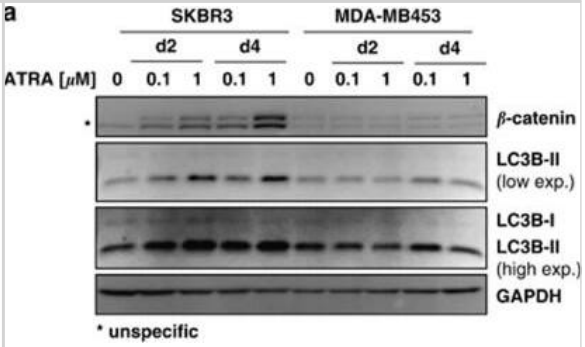

Endogenous MIR376A limits starvation-induced autophagy.(A) Blockage of endogenous MIR376A by Ant-376a, but not CNT-Ant further stimulated starvation (STV)-activated LC3-I to LC3-II conversion in MCF-7 cells. ACTB was used as a loading control. LC3-II/LC3-I densitometric ratios were marked. (B) Ant-376a, but not CNT-Ant resulted in further activation of SQSTM1 protein degradation following starvation in MCF-7 cells. SQSTM1/ACTB ratios were marked. Image collected and cropped by CiteAb from the following open publication (https://pubmed.ncbi.nlm.nih.gov/24358205), licensed under a CC-BY license. Not internally tested by Novus Biologicals.

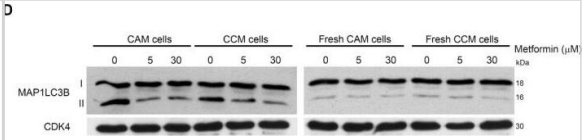

GAS6 increases the amount of both CIP2A and p-DAPK in RSC96 cells (A) RSC96 cells were incubated with GAS6 (100 ng/ml), and immunoblotting evaluations of CIP2A and p-DAPK expression were performed. The lower panel shows the intensity during basal conditions from the scanned imaged (upper panel). (B) RSC96 cells incubated with and without GAS6 (100 ng/ml) for 30 min and analysed by immunofluorescence. (C) Immunohistochemistry images demonstrated that CIP2A expression levels were higher than sham levels at 14 days and 28 days in the cavernous nerve after BCNI. Image collected and cropped by CiteAb from the following open publication (https://www.oncotarget.com/lookup/doi/10.18632/oncotarget.23978), licensed under a CC-BY license. Not internally tested by Novus Biologicals.

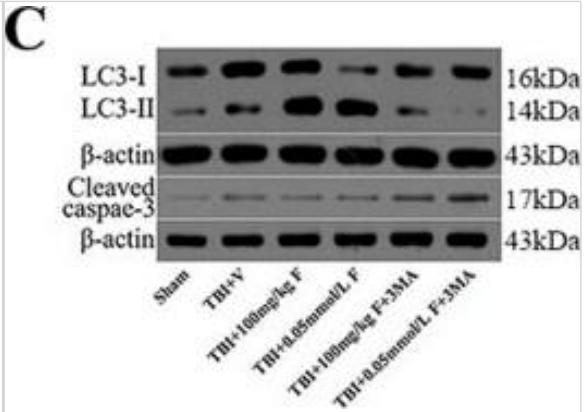

Effect of treatment with FX extract on CREB/BDNF signaling. (a-c) Differences in the phosphorylation of CREB and expression of BDNF between groups in the PFC and hippocampus (n = 3-4). (d, e) pCREB and BDNF immunofluorescence was assessed in the PFC and hippocampus (n = 3-4). Mean ± SD. #P < 0.05 versus normal group; □P < 0.05 and □□P < 0.01 versus control group. Scale bar = 200 μm. Image collected and cropped by CiteAb from the following open publication (https://pubmed.ncbi.nlm.nih.gov/30065945), licensed under a CC-BY license. Not internally tested by Novus Biologicals.

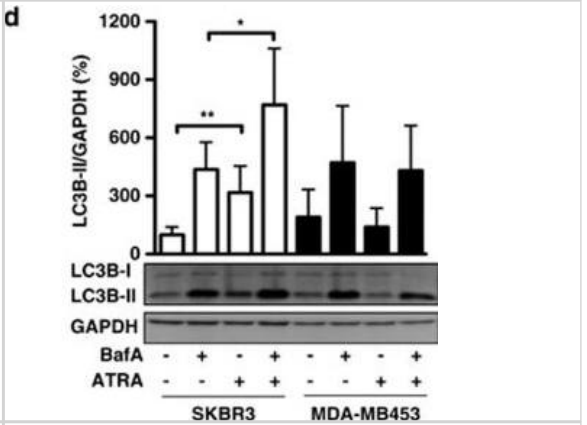

Immunohistochemistry of seven in absentia homolog 2 (SIAH2) gene in normal, in situ and invasive breast carcinomas. (A) Occasional nuclear positivity (arrows) in luminal cells in the terminal duct lobular unit. (B) Moderate to strong staining of SIAH2 in the nucleus of a small proportion of the cell in a high nuclear grade ductal carcinoma in situ with comedo necrosis. (C) Occasional weak to moderate SIAH2 (arrows) staining in a luminal type ductal carcinoma. (D) Strong SIAH2 staining in all nuclei in this basal-like breast carcinoma. Image collected and cropped by CiteAb from the following open publication (https://pubmed.ncbi.nlm.nih.gov/21306611), licensed under a CC-BY license. Not internally tested by Novus Biologicals.

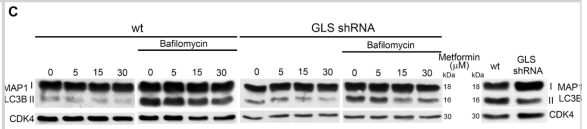

CNF1-triggered IL-1β maturation requires activated Rac, ASC and caspase-1.(A) Western blot analysis of the production and maturation/secretion of IL-1β by primary macrophages following treatment with CNF1, LPS or CNF1+LPS for 10 h. Actin and BSA were used as loading controls. (B) Quantification of caspase-1 activity in macrophages following treatment with CNF1+LPS for 6 h using YVAD-Fluorescent Labelled Inhibitor Caspase-1 Activity (FLICA). (C) Western blot analysis of macrophages IL-1β maturation/secretion upon transfection of HA-Rac2Q61E and LPS treatment. (D) Co-immunoprecipitation of Myc-Rac2 and caspase-1 using an anti-Myc antibody following the treatment of HEK 293T cells with CNF1+LPS for 6 h. Image collected and cropped by CiteAb from the following open publication (https://dx.plos.org/10.1371/journal.ppat.1004732), licensed under a CC-BY license. Not internally tested by Novus Biologicals.

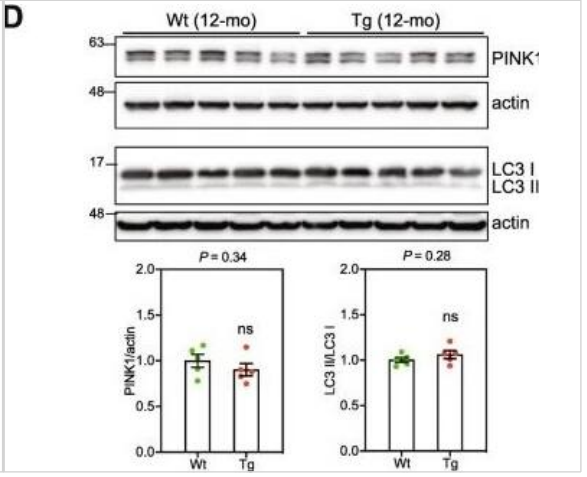

Expression of sphingosine-1-phosphate (S1P), interleukin (IL)-1β, and protease-activated receptor-1 (PAR-1) in isolated astrocytes. (A) Isolated and purified astrocytes were identified by bright-field microscopy and immunofluorescence for glial fibrillary acid protein (GFAP; red). Nuclei (DAPI) were labeled in blue. Scale bar = 100 μm. (B) Western blot and quantitative reverse transcription polymerase chain reaction (qRT-PCR) of the protein and mRNA expression, respectively, of S1P 0, 1, and 6 h after astrocytes were treated with lipopolysaccharide (LPS) or thrombin and Dabigatran (Dab) or PAR-1-inh (LPS only). (D) qRT-PCR and (E) enzyme-linked immunosorbent assay (ELISA) of the mRNA expression and secretion, respectively, of IL-1β 0, 1, and 6 h after astrocytes were treated with LPS or thrombin and Dab or PAR-1-inh (LPS only). (F) Immunofluorescence of astrocytes and quantification of relative mean integrated optical density (IOD; green fluorescence). PAR-1 was stained in green and nuclei (DAPI) were stained in blue. Scale bar = 100 μm. For (B–F), data are presented as the mean ± SD (n = 3). *p < 0.05; #p < 0.05 vs. the same group at 0 h; &p < 0.05 vs. the same group at 1 h. ns, not significant. Image collected and cropped by CiteAb from the following open publication (https://pubmed.ncbi.nlm.nih.gov/32694981), licensed under a CC-BY license. Not internally tested by Novus Biologicals.

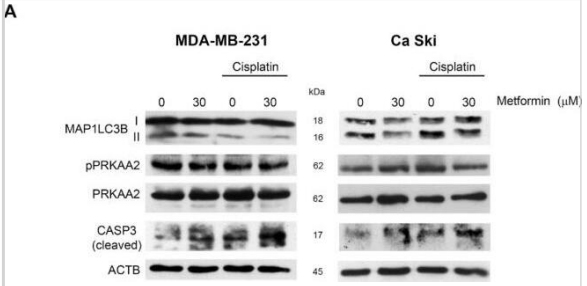

53BP1/RIF1 work epistatically to counteract BRCA1/CtIP-mediated end resection to regulate DSB repair pathway choiceA. HeLa cells harboring pGC were treated with the indicated siRNAs before transfection with I-SceI-expressing vector to induce DSBs. After 48h, the percentage of GFP+ cells was measured as an indication for HR efficiency. B.-D. Asynchronous A549 cells were treated with the indicated siRNAs before irradiation with 2Gy and CtIP B. and RPA foci C. were monitored at 2h while RAD51 D. foci were enumerated at 4h. E. Left panel: representative photos for the colocalization between 53BP1 and RIF1 foci in A549 cells at 2h after 2Gy. Right panel: quantitation of 53BP1, RIF1 or colocalized foci in the absence (DMSO) or presence of ATM inhibitor (ATMi). F. Left panel: representative micrographs for 53BP1 or RIF1 foci in irradiated cells after depletion of either proteins. Right panel: quantitation of experiments presented in the left panel. At least 100 nuclei were counted. In all cases, the number of foci measured in non-irradiated cells was subtracted (relative). Shown are the mean ±SEM for three independent experiments. sc: scrambled RNA, si53: si53BP1, siR: siRIF1, siB: siBRCA1, and siC: siCtIP. Image collected and cropped by CiteAb from the following open publication (https://www.oncotarget.com/lookup/doi/10.18632/oncotarget.11023), licensed under a CC-BY license. Not internally tested by Novus Biologicals.

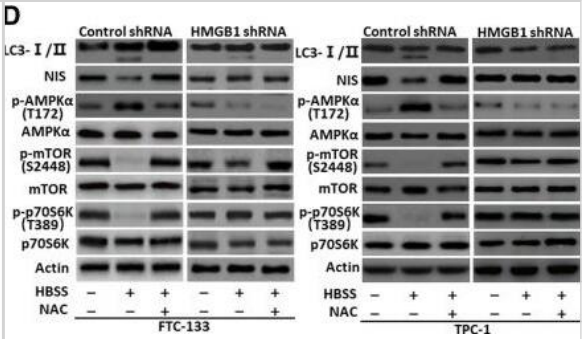

Up-regulation of RAS induced by cholesterol and 25-hydroxycholesterol in HK-2 cells. HK-2 cells were made quiescent by serum-free medium for 24 hours and then maintained in serum-free medium (control) or serum-free medium containing 30 μg/ml cholesterol together with 1 μg/ml 25-hydroxycholesterol (lipid) for 24 hours. (A) Real-time PCR of the total RAS components mRNA prepared from HK-2 cells with or without lipid treatment. AT1/AT2 ratio was evaluated as the balance between AT1 and AT2.β-actin was used as mRNA loading control. (B) Western blot analysis for RAS components protein expression. (C) The histogram shows the average volume density corrected by the housekeeping control, β-actin. Data is expressed as mean ± SD. *P < 0.05 vs. control. Angiotensinogen, AGT; angiotensin II, Ang II; angiotensin converting enzyme, ACE; angiotensin II type 1 receptor, AT1; angiotensin II type 2 receptor, AT2. Image collected and cropped by CiteAb from the following open publication (https://pubmed.ncbi.nlm.nih.gov/23570453), licensed under a CC-BY license. Not internally tested by Novus Biologicals.

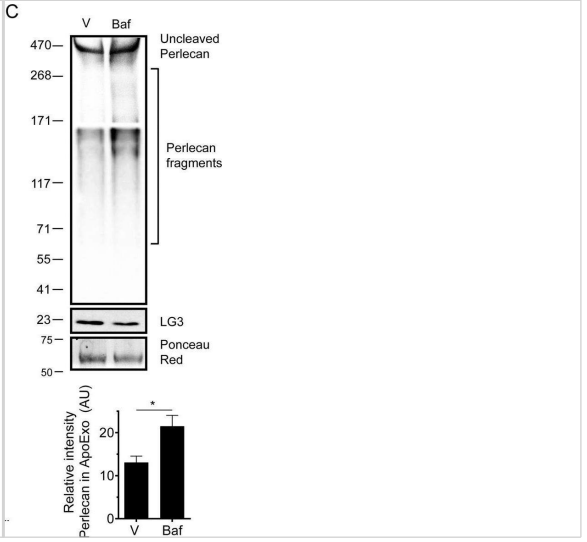

Effect of TERT silencing on murine M1 macrophage polarization.TERT siRNA and GV144-TERT were transiently transfected into LPS-treated RAW264.7 cells, respectively. (a) The endogeous TERT levels were detected by real-time PCR and western blot. The results are shown as relative expression against control expression without treatment. (b) The mRNA levels of M1 macrophages biomarkers including TNF-α, IL-1β, NOS2 and CCL2 were detected by real-time PCR. The results are shown as relative expression against control expression without treatment. (c) The secretion of proinflammatory cytokines including TNF-α, IL-1β, IL-6 and IL-12 were determined by ELISA. (d) TERT successful over-expression was verified by real-time PCR and western blot in LPS-stimulated RAW 264.7 cells. The results are shown as relative expression against control expression without treatment. (e) The mRNA levels of M1 macrophages biomarkers were detected by real-time PCR. The results are shown as relative expression against control expression without treatment. (f) The secretion of proinflammatory cytokines were determined by ELISA. Data shown are the mean ± SD from 3 independent experiments. *P < 0.05, **P < 0.01 vs control group. #P < 0.05, ##P < 0.01 vs LPS-treated group. Image collected and cropped by CiteAb from the following open publication (https://pubmed.ncbi.nlm.nih.gov/26725521), licensed under a CC-BY license. Not internally tested by Novus Biologicals.	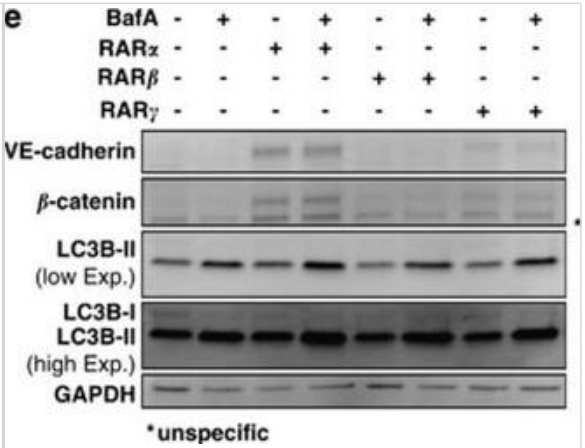
Ang II increases the number of TSP-1 positive cells in mouse heart and skin.IHC staining of TSP-1 was performed on paraffin sections from the heart (A) and skin (B) of PBS and Ang II treated WT mice. Representative photographs are shown from five animals per group. C. TSP-1 protein levels were increased in Ang II treated HDMECs in a dose dependent manner (*p≤0.05). Image collected and cropped by CiteAb from the following open publication (https://dx.plos.org/10.1371/journal.pone.0109763), licensed under a CC-BY license. Not internally tested by Novus Biologicals.	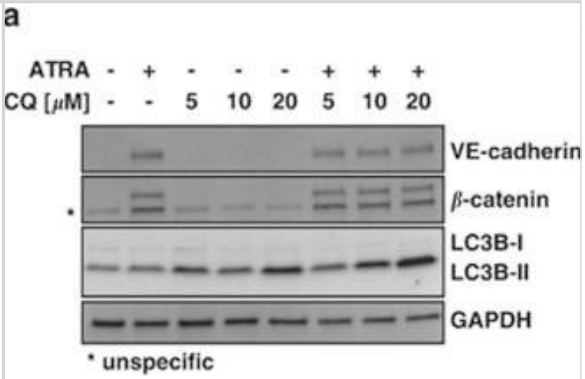

Publications

Toriyama K, Okuma T, Abe S et al. In vitro anticancer effect of azithromycin targeting hypoxic lung cancer cells via the inhibition of mitophagy Oncology letters 2024-01-01 [PMID: 38028184]

Zhang L, Hu Z, Bai W et al. Fucoxanthin ameliorates traumatic brain injury by suppressing the blood-brain barrier disruption iScience 2023-11-01 [PMID: 37965135] (IHC, WB, Mouse)

Details:
1:1000 dilution WB, 1:200 dilution IHC

Hurtado KA, Janda J, Schnellmann RG Lasmiditan restores mitochondrial quality control mechanisms and accelerates renal recovery after ischemia-reperfusion injury Biochemical pharmacology 2023-10-21 [PMID: 37866804] (WB, Mouse)

Bellanger D, Dziagwa C, Guimaraes C et al. Adipocytes Promote Breast Cancer Cell Survival and Migration through Autophagy Activation Cancers (Basel) 2021-08-03 [PMID: 34359819] (WB, B/N)

N Saito, J Araya, S Ito, K Tsubouchi, S Minagawa, H Hara, A Ito, T Nakano, Y Hosaka, A Ichikawa, T Kadota, M Yoshida, Y Fujita, H Utsumi, Y Kurita, K Kobayashi, M Hashimoto, H Wakui, T Numata, Y Kaneko, H Asano, M Odaka, T Ohtsuka, T Morikawa, K Nakayama, K Kuwano Involvement of Lamin B1 Reduction in Accelerated Cellular Senescence during Chronic Obstructive Pulmonary Disease Pathogenesis J. Immunol., 2019-01-28;0(0):. 2019-01-28 [PMID: 30692212] (B/N)

Khayati K, Bhatt V, Hu ZS et al. Autophagy compensates for Lkb1 loss to maintain adult mice homeostasis and survival eLife 2020-11-25 [PMID: 33236987] (WB)

Guo Y, Mao R, Xie Q et al. Francisella novicida Mutant XWK4 Triggers Robust Inflammasome Activation Favoring Infection Frontiers in Cell and Developmental Biology 2021-11-18 [PMID: 34869331] (WB)

Hoch L, Bourg N, Degrugillier F et al. Dual Blockade of Misfolded Alpha-Sarcoglycan Degradation by Bortezomib and Givinostat Combination Frontiers in Pharmacology 2022-04-27 [PMID: 35571097]

Tu YXI, Sydor AM, Coyaud E et al. Global Proximity Interactome of the Human Macroautophagy Pathway Autophagy 2022-05-04 [PMID: 34524948]

Castillo Bautista CM, Eismann K, Gentzel M et al. Obatoclax Rescues FUS-ALS Phenotypes in iPSC-Derived Neurons by Inducing Autophagy Cells 2023-09-11 [PMID: 37759469]

Koike T, Takenaka M, Suzuki N et al. Intracellular ferritin heavy chain plays the key role in artesunate-induced ferroptosis in ovarian serous carcinoma cells Journal of Clinical Biochemistry and Nutrition 2022-01-25 [PMID: 35903602] (WB)

Peugnet V, Chwastyniak M, Mulder P et al. Mitochondrial-Targeted Therapies Require Mitophagy to Prevent Oxidative Stress Induced by SOD2 Inactivation in Hypertrophied Cardiomyocytes Antioxidants (Basel) 2022-04-06 [PMID: 35453408]

More publications at http://www.novusbio.com/NB600-1384

Procedures

Western Blot protocol for LC3B Antibody (NB600-1384)

Protocol: Inhibition of Autophagy and LC3B Antibody (NB600-1384) Western Blot

Materials

Chloroquine diphosphate (CQ) (10 mM) in dH2O
1X PBS
Sample buffer, 2X Laemmli buffer: 4% SDS, 5% 2-mercaptoethanol (BME), 20% glycerol, 0.004% bromophenol blue, 0.125 M Tris HCl, pH 6.8
RIPA buffer: 150 mM NaCl, 1% NP-40 or Triton X-100, 0.5% sodium deoxycholate, 0.1% SDS, 50 mM Tris-HCl, pH 8.0, 20 mM Tris-HCl, pH 7.5
1X Running Buffer: 25 mM Tris-base, 192 mM glycine, 0.1% SDS. Adjust to pH 8.3
1X Transfer buffer (wet): 25 mM Tris-base, 192 mM glycine, 20% methanol, Adjust to pH 8.3
TBS
TBST, TBS and 0.1% Tween
Blocking solution: TBST, 5% non-fat dry milk
rabbit anti-LC3B primary antibody (NB100-2220) in blocking buffer (~2 ug/mL)

Methods

Tip: For more information on Western Blotting, see our Western Blot handbook.

1. Grow cells (e.g. HeLa or Neuro2A) in vitro to semi-confluency (70-75%).

2. Add CQ to culture dishes to a final concentration of 50 uM and incubate overnight (16 hours). Remember to include an untreated sample as a negative control.
Note: Validated autophagy inducers should be included as positive controls.

3. Rinse cells with ice-cold 1X PBS and lyse cells with sample buffer.
Note: LC3B-I and LC3B-II are sensitive to degradation, although LC3B-I is more labile. These proteins are sensitive to freeze-thaw cycles and SDS sample buffers. Fresh samples should be analyzed quickly to prevent protein degradation.

4. Sonicate and incubate cells for 5 minutes at 95oC.
Tip: Cells are lysed directly in sample buffer or may be lysed in RIPA buffer.

5. Load samples of Chloroquine-treated and -untreated cell lysates 40 ug/lane on a 4-20% polyacrylamide gradient gel (SDS-PAGE).
Tip: For detection of LC3B it is particularly important to monitor the progress of the gel as this protein is relatively small (~14kDa).

Tip: Alternatively, for non-gradient gels, use a 20% polyacrylamide gel.

6. Transfer proteins to a 0.2 um PVDF membrane for 30 minutes at 100V.

7. After transfer, rinse the membrane with dH2O and stain with Ponceau S for 1-2 minutes to confirm efficiency of protein transfer.

8. Rinse the membrane in dH2O to remove excess stain and mark the loaded lanes and molecular weight markers using a pencil.

9. Block the membrane using blocking buffer solution (5% non-fat dry milk in TBST) for 1 hour at room temperature.

10.Rinse the membrane with TBST for 5 minutes.

11.Dilute the rabbit anti-LC3B primary antibody (NB600-1384) (~2 ug/mL) in blocking buffer and incubate the

membrane for 1 hour at room temperature.

12.Rinse the membrane with dH2O.

13.Rinse the membrane with TBST, 3 times for 10 minutes each.

14.Incubate the membrane with diluted secondary antibody, according with product's specifications, (e.g. anti-rabbit-IgG HRP-conjugated) in blocking buffer for 1 hour at room temperature.
Note: Tween-20 may be added to the blocking or antibody dilution buffer at a final concentration of 0.05-0.2%, provided it does not interfere with antibody-antigen binding.

15.Rinse the membrane with TBST, 3 times for 10 minutes each.

16.Apply the detection reagent of choice (e.g. BioFX Super Plus ECL) in accordance with the manufacturer's instructions.

17.Image the blot.
Tip: LC3B-I and it's lipidated form LC3B-II have different electrophoretic mobility properties, with the lipidated form moving faster in an SDS-PAGE gel, albeit its larger molecular weight. LC3B-II runs at 14-16 kDa while LC3B-I runs at 16-18kDa.

Note: This assay measures the difference in the LC3B-II signal in the presence and absence of inhibitors (e.g., lysosomotropic agents). When autophagic flux is present or induced in a system an increase in the LC3B-II signal should be observed with the inhibitor.

Immunohistochemistry-Paraffin protocol for LC3B Antibody (NB600-1384)
LC3B Antibody:
Immunohistochemistry-Paraffin Embedded Sections

Antigen Unmasking:
Bring slides to a boil in 10 mM sodium citrate buffer (pH 6.0) then maintain at a sub-boiling temperature for 10 minutes. Cool slides on bench-top for 30 minutes.

Staining:
1. Wash sections in deionized water three times for 5 minutes each.
2. Wash sections in wash buffer for 5 minutes.
3. Block each section with 100-400 ul blocking solution for 1 hour at room temperature.
4. Remove blocking solution and add 100-400 ul diluted primary antibody. Incubate overnight at 4 C.
5. Remove antibody solution and wash sections in wash buffer three times for 5 minutes each.
6. Add 100-400 ul biotinylated diluted secondary antibody. Incubate 30 minutes at room temperature.
7. Remove secondary antibody solution and wash sections three times with wash buffer for 5 minutes each.
8. Add 100-400 ul Streptavidin-HRP reagent to each section and incubate for 30 minutes at room temperature.
9. Wash sections three times in wash buffer for 5 minutes each.
10. Add 100-400 ul DAB substrate to each section and monitor staining closely.
11. As soon as the sections develop, immerse slides in deionized water.
12. Counterstain sections in hematoxylin.
13. Wash sections in deionized water two times for 5 minutes each.
14. Dehydrate sections.
15. Mount coverslips.

Immunocytochemistry/Immunofluorescence Protocol for LC3B Antibody (NB600-1384)
Immunocytochemistry Protocol

Culture cells to appropriate density in 35 mm culture dishes or 6-well plates.

1. Remove culture medium and wash the cells briefly in PBS. Add 10% formalin to the dish and fix at room temperature for 10 minutes.
2. Remove the formalin and wash the cells in PBS.
3. Permeablize the cells with 0.1% Triton X100 or other suitable detergent for 10 min.
4. Remove the permeablization buffer and wash three times for 10 minutes each in PBS. Be sure to not let the specimen dry out.
5. To block nonspecific antibody binding, incubate in 10% normal goat serum from 1 hour to overnight at room temperature.
6. Add primary antibody at appropriate dilution and incubate overnight at 4C.
7. Remove primary antibody and replace with PBS. Wash three times for 10 minutes each.
8. Add secondary antibody at appropriate dilution. Incubate for 1 hour at room temperature.
9. Remove secondary antibody and replace with PBS. Wash three times for 10 minutes each.
10. Counter stain DNA with DAPi if required.

Novus Biologicals USA
10730 E. Briarwood Avenue
Centennial, CO 80112
USA
Phone: 303.730.1950
Toll Free: 1.888.506.6887
Fax: 303.730.1966
nb-customerservice@bio-techne.com

Bio-Techne Canada
21 Canmotor Ave
Toronto, ON M8Z 4E6
Canada
Phone: 905.827.6400
Toll Free: 855.668.8722
Fax: 905.827.6402
canada.inquires@bio-techne.com

Bio-Techne Ltd
19 Barton Lane
Abingdon Science Park
Abingdon, OX14 3NB, United Kingdom
Phone: (44) (0) 1235 529449
Free Phone: 0800 37 34 15
Fax: (44) (0) 1235 533420
info.EMEA@bio-techne.com

General Contact Information
www.novusbio.com
Technical Support: nb-technical@bio-techne.com
Orders: nb-customerservice@bio-techne.com
General: novus@novusbio.com

Products Related to NB600-1384

NB820-59177	Human Brain Whole Tissue Lysate (Adult Whole Normal)
HAF008	Goat anti-Rabbit IgG Secondary Antibody [HRP]
NB7160	Goat anti-Rabbit IgG (H+L) Secondary Antibody [HRP]
NBP2-24891	Rabbit IgG Isotype Control

Limitations

This product is for research use only and is not approved for use in humans or in clinical diagnosis. Primary Antibodies are guaranteed for 1 year from date of receipt.

For more information on our 100% guarantee, please visit www.novusbio.com/guarantee

Earn gift cards/discounts by submitting a review: www.novusbio.com/reviews/submit/NB600-1384

Earn gift cards/discounts by submitting a publication using this product: www.novusbio.com/publications